Modeling of Radiative Heating in Base Region of Jovian Entry Probe

Chul Park

Reprinted from **Entry Heating and Thermal Protection**, *edited by Walter B. Olstad, Vol. 69 of Progress in Astronautics and Aeronautics.*

MODELING OF RADIATIVE HEATING IN BASE REGION OF JOVIAN ENTRY PROBE

Chul Park*
Ames Research Center, NASA, Moffett Field, Calif.

Abstract

A theoretical model is derived to determine the average thermodynamic properties in the expanding region, recirculating region, recompression region, and neck region through application of one-dimensional conservation equations. Radiative transfer is calculated using spectrally detailed computer codes accounting for nonequilibrium. The results show that the most severe heating occurs immediately behind the frustum, and that the recompression and neck regions are the major sources of radiation that heats the base stagnation point, The radiation flux to the base point is slightly stronger with ablation than without. Its value is $0.11(43p_b/p_s)^2$ times that to the front stagnation point where the base pressure p_b is defined as the average pressure in the recirculating region and p_s is the front stagnation-point pressure. The time-integrated heat load to the base point is $18(43p_b/p_s)^2$ kJ/cm^2.

Nomenclature

e = radiative power emission from unit volume
H = total enthalpy
h = static enthalpy
$\dot{M}$ = mass flow rate through neck
N_e = electron density
p_b = average pressure in base region
p_s = front stagnation-point pressure
q = radiative heat-transfer rate to a base point
q_s = radiative heat-transfer rate to front stagnation point
R_f = frustum radius
R_n = neck radius

Presented as Paper 79-0039 at the AIAA 17th Aerospace Sciences Meeting, New Orleans, La., Jan. 15-17, 1979. This paper is declared a work of the U. S. Government and therefore is in the public domain.

*Research Scientist.

r = radius
T_e = electron temperature
t = time
u = tangential velocity
u_e, = velocity at outer ec
u_e = velocity at outer ec
x = distance along cente
x_n = distance between rea
Y = coordinate normal tc
Δ = shock standoff dista
δ = thickness of layer (by free-shear laye
λ = wavelength of radiat
ρ = density
θ = viewing angle measur
$(\bar{})$ = volume average

In a future space mis
be flown into the atmosphe
transfer to the probe vehi
radiation. Up to the pres
heat-transfer problem focu
vehicle where the heat-tra
important. Little effort
heat-transfer rate to the
region. Existing reports
transfer rate to the base
the front stagnation point
heat-transfer to the base
radiation is the dominant
body region, one should ex
region. The present work
retically the radiative he

The problem of radiat
by Stephenson.[2,3] He meas
behind a model flying thro
tion sensors located outsi
consisted of air, and the
by molecular dissociation.
fore of a molecular nature
rate of the base region of
the sensor location from o
carrying out the associate
The radiative heat-transfe
about 90 W/cm^2 under his t
rate is calculated to be e

r = radius
T_e = electron temperature
t = time
u = tangential velocity
u_e = velocity at outer edge of free-shear layer
$u_{e'}$ = velocity at outer edge of neck
x = distance along centerline axis
x_n = distance between reattachment point and frustum edge
Y = coordinate normal to flow direction
Δ = shock standoff distance
δ = thickness of layer (in shock layer) eventually entrained by free-shear layer
λ = wavelength of radiation
ρ = density
θ = viewing angle measured at base stagnation point
$(\bar{\ })$ = volume average

Introduction

In a future space mission, a probe vehicle is planned to be flown into the atmosphere of the planet Jupiter. Heat transfer to the probe vehicle is expected to be due mostly to radiation. Up to the present, most studies of the radiative heat-transfer problem focused on the forebody region of the vehicle where the heat-transfer problem is undoubtedly more important. Little effort has been expended to determine the heat-transfer rate to the afterbody, that is, to the base region. Existing reports indicate that the convective heat-transfer rate to the base region is typically 1% of that to the front stagnation point.[1] Unknown, however, is the rate of heat-transfer to the base region by radiation. Since radiation is the dominant mode of energy transport in the forebody region, one should expect the same for the afterbody region. The present work is an attempt to determine theoretically the radiative heat-transfer rate to the base region.

The problem of radiative base heating was studied first by Stephenson.[2,3] He measured the luminosity of the trail behind a model flying through a free-flight range with radiation sensors located outside the model. The ambient gas consisted of air, and the flow around the model was dominated by molecular dissociation. The radiation observed was therefore of a molecular nature. He deduced the radiative heating rate of the base region of the model by hypothetically moving the sensor location from outside to inside the model and by carrying out the associated geometrical-optics calculations. The radiative heat-transfer rate was determined to be up to about 90 W/cm^2 under his test conditions.[2] This heat-transfer rate is calculated to be equivalent to about 1/3 that to the

front stagnation point. The experiment showed that the neck region (i.e., the region around and immediately downstream of the reattachment point) and the expanding region behind the shoulder (hereafter referred to as shoulder-expansion region) are highly luminous. In a later unpublished preliminary calculation communicated internally within NASA, Stephenson recognized the recirculating region adjacent to the base wall to be a major contributor to base heating because, even though it is less luminous than the other two regions, it is closer to the base wall. Thus, three important sources of radiation are identified: the shoulder-expansion region, the recirculating region, and the neck region.

Recently, Shirai and Park[4] measured the radiative base heating rate with radiation sensors imbedded in the model in a shock-tube flow. The flow was in an ionizing regime, and the radiative heat-transfer rate to the base stagnation point was found to be on the order of 1 kW/cm^2, or 10% of that to the front stagnation point. The luminosity photographs of the flow field obtained by Shirai and Park showed the same features as seen by Stephenson. A theoretical analysis is required, however, to extrapolate their experimental results to the full-scale case since the tests did not simulate the correct flight Mach numbers or the size.

An attempt was made recently by Nestler and Brant[5] to determine theoretically the heat-transfer rate to the base region of the Jovian probe. Through a detailed analysis of the flow field in the recirculating region, they calculated the convective heat-transfer rate for the base region to a relatively high precision. Only preliminary results are presented in their work, however, on the radiative contribution, which is not adequate for the purpose of spacecraft design.

The present analysis complements the work of Nestler and Brant.[5] It makes use of simple one-dimensional conservation equations to determine the average thermodynamic properties in the luminous regions. Radiative-transfer calculations are carried out using spectrally detailed computer codes accounting for the effect of nonequilibrium in the shoulder-expansion region. The theoretical model qualitatively reproduces the features found experimentally by Stephenson[2,3] and Shirai and Park.[4] The calculation is carried out for the full-scale Jovian probe configuration, which consists of a 45° sphere cone with a nose radius of 31.12 cm and a frustum radius of 62.24 cm. The base wall of the vehicle also is spherical (radius of 62.24 cm), with the base stagnation point 34.9 cm downstream of the plane of the frustum edge. The flow environments considered are those encountered in a -9° entry

calculated by Moss et al. heating rates of the base immediately behind the fr

Met

Shoulder-Expansion Region

Analysis of base flo region. Provided the ini over the frustum) and the between the expansion reg known, it would seem poss flow numerically by using it is very difficult to d radiation, and chemical n

To provide an altern region flow field, a free Research Center. In expe field, one important para boundary-layer thickness theoretical and experimen dictates the dynamics of nonablating cases.[7,8] Th Mach number and body geom

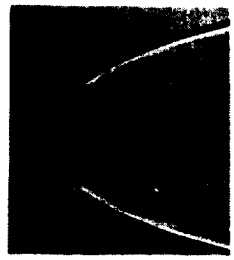

a) Velocity =

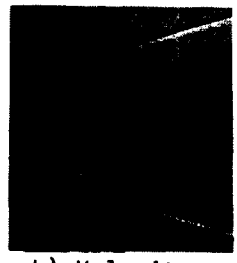

b) Velocity =

Fig. 1 Free

calculated by Moss et al.[6] The analysis derives the radiative heating rates of the base stagnation point and of the region immediately behind the frustum.

Method of Solution

Shoulder-Expansion Region

Analysis of base flow starts from the shoulder-expansion region. Provided the initial conditions (i.e., the flow field over the frustum) and the geometry of the free-shear layer between the expansion region and the recirculating region are known, it would seem possible in principle to solve for the flow numerically by using existing techniques.[7] In practice it is very difficult to do so because of ablation,[8] radiation, and chemical nonequilibrium.

To provide an alternative way to determine the base region flow field, a free-flight test was performed at Ames Research Center. In experimentally simulating the base flow field, one important parameter is believed to be the ratio of boundary-layer thickness to shock-layer thickness. Existing theoretical and experimental evidence indicates that this ratio dictates the dynamics of base flow field in both ablating and nonablating cases.[7,8] This ratio depends, in turn, for a given Mach number and body geometry, mainly on the effective

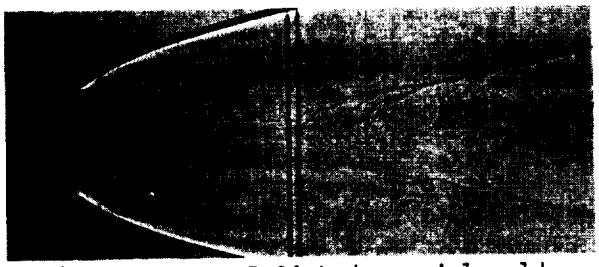

a) Velocity = 5.34 km/s, model cold.

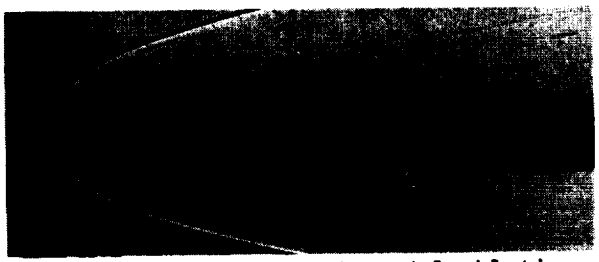

b) Velocity = 5.22 km/s,model ablating.

Fig. 1 Free-flight shadowgraph.

specific heat ratio γ prevailing in the forebody shock layer and the characteristic Reynolds number. In the Ames experiment, therefore, an attempt was made to reproduce these two parameters. An iron scale model of the Jovian probe, 2.03 cm diam, was flown in an ambient atmosphere consisting of 39% oxygen and 61% argon by volume at 122 Torr, at a velocity of 5.3 km/sec. The mixture produced a specific heat ratio γ between 1.2 and 1.4 in the forebody region, a fair simulation of the Jovian flight conditions. The solutions by Moss et al.[6] show γ to vary from 1.1 at the wall to about 1.3 at the shock. The test also produced a Reynolds number that agrees closely with that in the Jovian flight case. Shadowgraph pictures were taken at several stations along the flight path. Two such photographs, one taken at an upstream station where the model is cold and the other at a downstream station where the model is ablating, are shown in Figs. 1 a and 1 b . The shadowgraphs show the following features:

(1) For the nonablating case, the angle of the free-shear layer, as judged by the line of demarcation caused by the temperature gradient along the layer, is -11.5° on the average.

(2) For the nonablating case, the neck is located about 1.5 diam downstream of the frustum.

(3) The diameter of the neck is about 2/3 that of the body diameter for both ablating and nonablating cases. Here the neck radius is defined as the extreme outer edge of the domain containing the ablation product.

In addition to these features, the present analysis makes use of the results of Stephenson[2] which showed that, for the ablating case, the location of the neck is at 1.5 body diam downstream of the frustum. One notices here that some of Stephenson's luminosity photographs show the neck radius to be about half the body radius rather than 2/3 of the radius. However, this can be attributed to photographic deception: the weak luminosity of the edge of the neck could be below the lower cutoff of the photographic sensitivity.

A method-of-characteristics calculation was carried out by the present author for the shoulder-expansion region, assuming the gas to be perfect with $\gamma = 1.2$. The γ value was chosen because (1) it is an average between the values at the wall and the shock wave and (2) it is approximately the largest γ value for which the method of characteristics is practical. (At higher γ values, the flow over the frustum becomes subsonic, thereby rendering the method invalid.) The shear layer was replaced by a straight backward-facing cone of -11.5° half-angle for this calculation (see Fig. 2 a). From

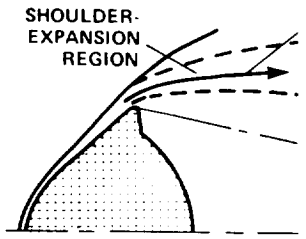

a) Stream tube for lumino
region.

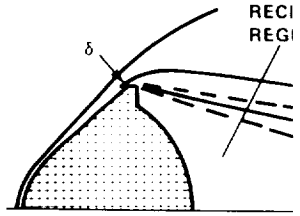

b) Ve

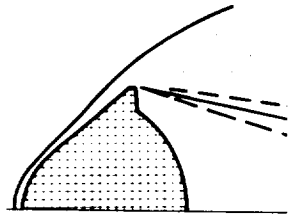

c) Stati

Fig. 2 Schem

the solution, a stream tul
of maximum pressures and
radiation intensity increa
it will be the strongest
thickness of the stream t
shock-layer thickness at
to be a mixture only of h
ablation product gases are
The present choice of repr
overestimate pressure and
radiation power emitted by
the shock layer. This ter
partly, by the fact that
portion that came past the
neglected in the radiatior

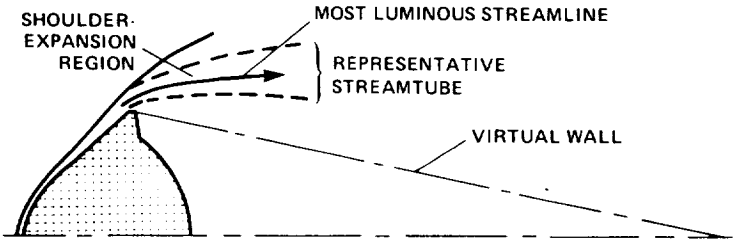

a) Stream tube for luminosity calculation in shoulder-expansion region.

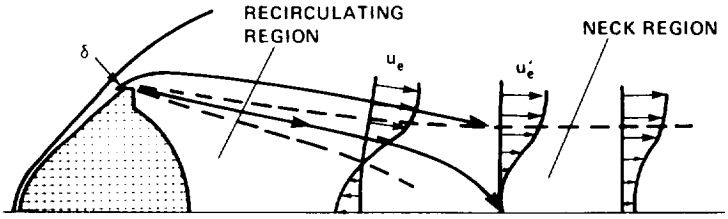

b) Velocity profile.

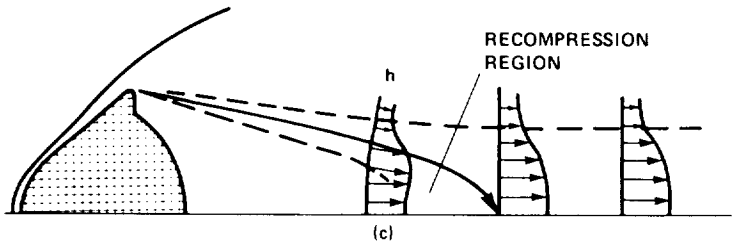

c) Static enthalpy profile.

Fig. 2 Schematic of base flow field.

the solution, a stream tube was chosen which is along the path of maximum pressures and temperatures (see Fig. 2 a). Because radiation intensity increases with pressure and temperature, it will be the strongest along this streamline. The initial thickness of the stream tube is taken to be (outer) 80% of the shock-layer thickness at the frustum edge. The gas is assumed to be a mixture only of hydrogen and helium; concentration of ablation product gases are most likely to be negligibly small. The present choice of representative stream tube tends to overestimate pressure and temperature on the average and hence radiation power emitted by the gas mass that passed through the shock layer. This tendency is compensated for, at least partly, by the fact that the flow region above, that is, the portion that came past the extended bow shock wave, is neglected in the radiation calculation.

Flow properties are then calculated along this representative stream tube using a computer code for hydrogen-helium mixture developed by the present author which accounts for finite-rate ionic reactions of hydrogen ions and electrons and nonequipartition of energies between electrons and heavy particles.[9] The calculation uses the pressure variation specified by the method-of-characteristics solution. Radiation power emitted by the stream tube is then calculated using the method to be described later (see the section on Radiation).

Recirculating and Recompression Regions

To calculate radiative properties in the recirculating region, one must first determine the static pressure in the region. It is known that pressure varies considerably within the region between the body surface and the neck reattachment point. It is generally low near the body surface, the lowest point being at a point a short distance away from the base stagnation point.[8] Existing experimental evidence,[8] the theory of Weng and Chow,[7] and the recent unpublished calculations made at Ames Research Center indicate that pressure rises almost linearly with axial distance, starting from a point about one body radius away from the stagnation point. Traditionally, base pressure is defined as the pressure at the base stagnation point.[5,10] This pressure value is appropriate in calculating convective heat-transfer rates. Since radiative emission occurs mainly in the high-pressure region away from the surface, however, this traditional base pressure value is of little consequence in the present problem.

In the present work, the region between the body surface and the neck point is divided arbitrarily into a "recirculating region" and a "recompression region." The recirculating region is considered to extend from the body surface to 2/3 of the distance from the surface to the neck point. For the purpose of simplifying radiation calculations, pressure was assumed to be constant in each of the two regions. These pressure values, which are the bulk average values in the regions, are estimated from the following procedure:

From the turning angle around the frustum edge obtained from the free-flight tests, one can calculate the pressure behind the frustum edge using the Prandtl-Meyer expansion method. The flow-turning angle is first determined by subtracting the sonic-point angle, which is the angle of the body surface where the flow reaches sonic velocity, from the angle of the free-shear layer. Pressure change is then determined assuming that the flow process follows Prandtl-Meyer expansion over the turning angle. For the nonablating case

with $\gamma = 1.3$, the soni
and hence the turning
to a base-to-front sta
The average pressure i
be the algebraic avera
recirculating region a
using the method descr

It is to be notec
value adopted in the p
traditional base press
0.8% of the front stag
is adopted, the Mach r
becomes close to 5. L
finds the neck pressur
value.[8] Since static
linearly with distance
from the surface), the
circulating region bec
of the front stagnatic

The second import
of radiative propertie
enthalpy, one examines
circulating and recomp
the dividing streamlin
edge velocity u_e (velo
layer, see Ref. 8). T
along the centerline a
For the purpose of cal
average velocity in th
is, the algebraic aver
velocity in the region
culated as

$$\bar{h} = \bar{H} -$$

This approximation int
the radiation calculat
the region is a small
enthalpy.

The average total
recompression regions
layer allows rapid tra
enthalpy across it, th
will be almost uniform
of the flow mass entra
reduces, therefore, to

with $\gamma = 1.3$, the sonic speed is reached at the frustum edge and hence the turning angle is $45° + 11.5° = 56.5°$. This leads to a base-to-front stagnation-point pressure ratio of 0.023. The average pressure in the recompression region is taken to be the algebraic average between the average pressure in the recirculating region and the neck pressure which is determined using the method described later.

It is to be noted here that the average base pressure value adopted in the present work is consistent with the traditional base pressure value which is known to be about 0.8% of the front stagnation-point value.[5] If the 0.8% value is adopted, the Mach number in the shoulder expansion region becomes close to 5. Using the Chapman-Korst theory, one then finds the neck pressure to be at least 10 times the 0.8% value.[8] Since static pressure increases approximately linearly with distance (starting from one body radius away from the surface), the volume-averaged pressure in the recirculating region becomes nearly equal to or greater than 2% of the front stagnation-point value.

The second important parameter needed in the determination of radiative properties is static enthalpy. To determine the enthalpy, one examines velocity distribution within the recirculating and recompression regions (see Fig. 2 b). Along the dividing streamline, velocity is approximately half the edge velocity u_e (velocity at the outer edge of the free-shear layer, see Ref. 8). The maximum velocity of the reverse flow along the centerline axis is also approximately $u_e/2$ (Ref. 8). For the purpose of calculating radiative properties, the average velocity in the region u is assumed to be $u_e/4$, that is, the algebraic average between the maximum and minimum velocity in the region. The average static enthalpy is calculated as

$$\bar{h} = \bar{H} - (1/2)\bar{u}^2 = \bar{H} - (1/2)(u_e/4)^2$$

This approximation introduces only a small uncertainty into the radiation calculation because the average kinetic energy in the region is a small fraction (about 3%) of the total enthalpy.

The average total enthalpy $\bar{H}$ within the recirculating and recompression regions must now be determined. Since the shear layer allows rapid transport of mass, momentum, and total enthalpy across it, the total enthalpy H within the regions will be almost uniform and equal to the average total enthalpy of the flow mass entrained into the shear layer. The problem reduces, therefore, to that of determining the average total

enthalpy of the flow entrained by the shear layer. The mass entrained by the shear layer originates in the lower portion of the shock layer, indicated in Fig. 2 a by $0 < Y < \delta$. If δ is known, the average total enthalpy H is determined as

$$\bar{H} = \int_0^{\delta} \rho u H \, dY \Big/ \int_0^{\delta} \rho u \, dY$$

The point δ is determined in the present work by imposing the requirement that the calculated neck radius equals the value observed experimentally. The details of the method are explained in the following section.

The average enthalpy $\bar{H}$ is used also in determining the shear-layer edge velocity u_e. The process of expansion from the frustum edge to the edge of shear layer is represented by a stream tube. The pressure variation along this stream tube is assumed to be such that pressure reaches the average base pressure p_b within about 15 cm from the frustum edge. For the hypothetical case of no ablation calculated by Moss,[6] the non-equilibrium one-dimensional flow code for hydrogen-helium mixture used for the shoulder-expansion region is used here also to determine the edge velocity u_e. The resulting u_e value is found to correspond to about 50% of the total enthalpy, which is substantially smaller than that obtained under the assumption of equilibrium flow. For the case with ablation, similar calculation is presently impractical because the rate coefficients associated with the reactions involving carbonaceous species are unknown. The velocity u_e is determined for this case, therefore, assuming that 50% of the total enthalpy is converted to kinetic energy, as is found to be the case for the nonablating case.

Since the flow velocity is relatively slow in the recirculating and recompression regions, and since the length over which the gas therein must travel is long, it is likely that thermodynamic equilibrium prevails within the region. From the pressure and static enthalpy values determined previously, therefore, temperature and concentrations of each chemical species are determined uniquely via an equilibrium thermochemistry calculation. Radiative properties of the region are then determined by the method described later. For the purpose of radiative-transfer calculations, the shape of the recirculating and decompression regions is taken to be a truncated cone of 11.5° half-angle.

Neck Region

The dividing streamline converges into a reattachment point where velocity is zero. Since the dividing streamline

meets the centerline a
axial velocity profile
to radius, as shown sc
low velocity constitute
mass entrained in the
cross-sectional area o
the shear layer because
the neck. The velocity
mated in the present w

The flow velocity at t
determined from the as
corresponding to the P
be 0.92 u_e.

From the velocity
profile is constructed
enthalpy in the neck is
and recompression regio
the same entrainment pr
layer. As was done for
regions, the radiative
determined by assuming
uniform at the average
average kinetic energy
average kinetic velocit
assumed velocity profil

$$\pi R_n^2 \bar{u}^2 = 2$$

Static pressure is
the free-shear layer.
steady. As the flow ap
pressure rises graduall
pressure and, to a less
the flow field, that is
The pressure rise due t
function mostly of the
about 3 in the present
theoretical data indica
pressure at the reattac
times that outside the
flow.[7,8,12] (At a high
correspondingly larger.
an isentropic compressi
dimensional, Prandtl-Me

meets the centerline axis at a right angle at this point, the axial velocity profile has zero first derivative with respect to radius, as shown schematically in Fig. 2 b . The region of low velocity constitutes a "neck" through which the entire flow mass entrained in the shear layer must pass.[11] The overall cross-sectional area of the neck is much larger than that of the shear layer because the average flow velocity is slow in the neck. The velocity profile across the neck is approximated in the present work by the quadratic expression:

$$u = u_e'(r/R_n)^2$$

The flow velocity at the outer edge of the neck, u_e', is determined from the assumption of isentropic compression corresponding to the Prandtl-Meyer turning angle of 11.5° to be 0.92 u_e.

From the velocity profile obtained, the static enthalpy profile is constructed (Fig. 2 c). The average total enthalpy in the neck is the same as that in the recirculating and recompression regions because all three regions are fed by the same entrainment process occurring in the free shear layer. As was done for the recirculating and recompression regions, the radiative properties in the neck region are determined by assuming that the static enthalpy therein is uniform at the average value determined by subtracting the average kinetic energy from the average total enthalpy. The average kinetic velocity $\bar{u}$ is calculated in turn from the assumed velocity profile as

$$\pi R_n^2 \bar{u}^2 = 2\pi \int_0^{R_n} ru^2 dr = (\pi/16) R_n^2 u_e'^2$$

Static pressure is almost constant in the early stage of the free-shear layer. The edge velocity u_e is correspondingly steady. As the flow approaches the reattachment point, pressure rises gradually due mostly to recovery of dynamic pressure and, to a lesser extent, by virtue of axisymmetry of the flow field, that is, narrowing of cross-sectional area. The pressure rise due to recovery of dynamic pressure is a function mostly of the Mach number of the edge flow, which is about 3 in the present case. Existing experimental and theoretical data indicate that, at a Mach number of 3, the pressure at the reattachment point is slightly under three times that outside the shear layer for the two-dimensional flow.[7,8,12] (At a higher Mach number, the ratio is correspondingly larger.) A similar value is obtained through an isentropic compression calculation — an inverse two-dimensional, Prandtl-Meyer calculation corresponding to the

turning angle of 11.5° gives a pressure rise factor of 2.8. Existing literature indicates that axisymmetry adds slightly to this pressure rise.[7] The present work assumes therefore that the pressure in the neck region is three times the average base pressure.

Since the average velocity is relatively slow and the pressure is high, thermodynamic equilibrium is expected to be established within the neck region. From the average enthalpy and pressure values obtained, therefore, one can determine the rest of the state properties through an equilibrium thermochemistry calculation. Using the average density $\bar{\rho}$ thus obtained, the mass flow rate through the neck $\dot{M}$ is calculated as

$$\dot{M} = 2\pi\bar{\rho} \int_0^{R_n} ru \, dr = (1/2)\, \pi R_n^2 \bar{\rho} u_e'$$

By requiring that the calculated neck radius R_n equals the value observed experimentally, that is,

$$R_n = (2/3)R_f$$

$\dot{M}$ is uniquely determined. From the $\dot{M}$ value, the thickness of the inner shock layer swallowed by the shear layer, δ (Fig. 2 b) is determined from the relation

$$\dot{M} = 2\pi R_f \int_0^{\delta} \rho u \, dY$$

From the value of δ determined in this way, one can calculate the average total enthalpy $\bar{H}$ needed to determine the static enthalpy values for both the recirculating/recompression region and the neck region using the method described earlier. The calculation is carried out in a trial-and-error manner. An arbitrary value of δ is first assumed, and the corresponding value of R_n is calculated from it. The R_n value is then compared with the experimental value, and the parameter δ is adjusted until the calculated R_n agrees with the observed value.

Downstream of the neck, the flow accelerates gradually because of the shear force exerted on it by the outside flow. In return, the outer flow is accelerated and is entrained in the inner region. The flow thus evolves into a wake. Typical velocity profiles and enthalpy profiles in the early stage of the wake are shown in Figs. 2 b and 2 c .

Experimental data of Stephenson[2,3] show that the high luminosity of the neck region extends over approximately 1

body diameter. In the re
luminosity attenuates gra
calculation, the neck-plu
a cylinder of uniform lum
neck radius and a length

Radiation

The foregoing calcul
carried out for the Jovia
Moss et al.[6] The base-fl
six entry trajectory poin
of zero ablation and one
benchmark point is approx
(for the front stagnation
with finite ablation is ob
shield, assuming the ablat
shock-layer profiles gene
determining the average t
centrations in the base re
pressure is assumed to be
pressure which is derived

The radiative transfe
both the nonequilibrium re
expansion region) and the
recompression, and neck re
region, the species contri
hydrogen (H) and ionized h
ablation products and radi
weak. For the equilibrium
calculations are carried o
the hypothetical zero abla
containing ablation produc
oxygen, and their molecula

For the nonequilibriu
properties can be calculat
computer code NEQRAP.[13] T
equilibrium population of
date techniques and accoun
broadening of hydrogen lin
calculation with a slight
excited hydrogen atoms is
the free (i.e., ionized) s
represents a variation fro
dynamic equilibrium) approx
pseudo-LTE approximation,[1
rigorous solutions yield ex

body diameter. In the region downstream of the bright region, luminosity attenuates gradually. For the purpose of radiation calculation, the neck-plus-wake region is represented here by a cylinder of uniform luminosity having a radius equal to the neck radius and a length equal to 1.5 body diameters.

Radiation

The foregoing calculation of base-flow parameters is carried out for the Jovian entry environments calculated by Moss et al.[6] The base-flow calculations are carried out for six entry trajectory points under the hypothetical assumption of zero ablation and one benchmark point with ablation. The benchmark point is approximately at the peak heating point (for the front stagnation point). The benchmark calculation with finite ablation is obtained for a carbon-phenolic heat shield, assuming the ablation layer to be turbulent. The shock-layer profiles generated by Moss's solutions are used in determining the average total enthalpies and species concentrations in the base region. The volume-averaged base pressure is assumed to be 2.3% of the front stagnation-point pressure which is derived for the nonablating case for γ 1.3.

The radiative transfer calculation is carried out for both the nonequilibrium region behind the frustum (shoulder-expansion region) and the equilibrium region (recirculating, recompression, and neck regions). For the nonequilibrium region, the species contributing to radiation are neutral hydrogen (H) and ionized hydrogen (H^+). The flow contains no ablation products and radiation from helium is negligibly weak. For the equilibrium regions along the axis, radiation calculations are carried out for both the $H+H_e$ mixture (for the hypothetical zero ablation condition) and for the mixture containing ablation products (hydrogen, helium, carbon, oxygen, and their molecular compounds and ions).

For the nonequilibrium ionized hydrogen, radiative properties can be calculated to a high precision using the computer code NEQRAP.[13] The code calculates the non-equilibrium population of excited states using the most up-to-date techniques and accounts rigorously for the Stark broadening of hydrogen lines. The code is used in the present calculation with a slight modification: the population of excited hydrogen atoms is assumed to be in equilibrium with the free (i.e., ionized) state. This assumption, which represents a variation from the popular LTE (local thermodynamic equilibrium) approximation and hence can be termed a pseudo-LTE approximation,[13] is based on the finding that the rigorous solutions yield excited state populations that are

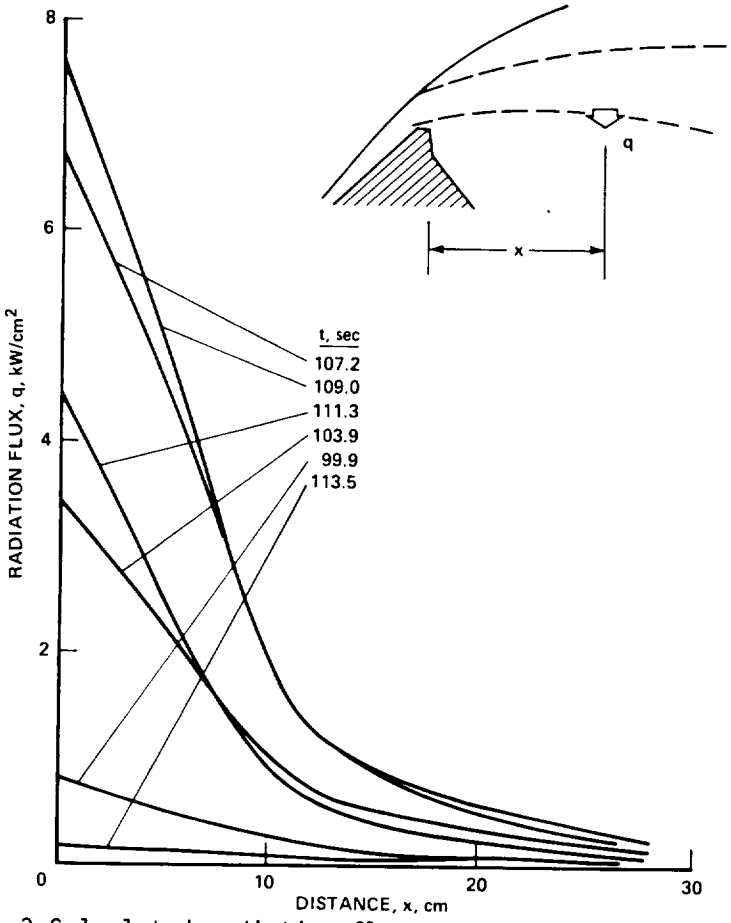

Fig. 3 Calculated radiation flux emerging from shoulder-expansion region.

very close to those obtained from the pseudo-LTE approximation. The largest deviation of the pseudo-LTE value from the rigorous population value, which is still under 10%, occurs for the first excited state from which the Lyman-alpha line emanates. But since the Lyman-alpha line is mostly self-absorbed, inaccuracy of its population value does not lead to significant error. For the second excited state and higher states, which produce Balmer and Paschen lines and hence contribute significantly, deviation of the pseudo-LTE values from the rigorous solutions is less than 2%. The calculation procedure adopted in the present work is believed to be accurate, therefore, to within about 2% in the radiation properties. The photon energy range of 0.2 to 16.2 eV is divided into 3000 equally spaced intervals for the calculation.

A one-dimensional
adopted for the calcula
shoulder-expansion regi
is calculated only in t
the centerline axis, an
multiplying the intensi
cedure implicitly assur
thinner than the body d
optically thin for the
The assumptions are bel
of 10%, which is accept

For the three equi
central axis (recircula
an axisymmetric radiati
for the base stagnation
falling on the stagnati
function of the viewing
formed along 16 differe
are chosen at especiall
resolve the rapidly var
the neck region. Radia
lation are obtained usi

For the case with
the code ARCRAP indicat
negligible for the benc
is above 10,000 K in al
molecules are very smal
oxygen species are seen
species contributing si
therefore, are hydrogen
properties of hydrogen
neutral carbon included
listed in the NBS table
used for these lines) ar
upper state of principal
missing from the NBS tab
obtained from the corre

Altogether 374 line
the carbon lines is take
Gaussian component of th
from temperature. The L
profile consists of thre
natural broadening, Star
broadening. The width c
exactly. All Stark line

A one-dimensional radiative transfer approximation is adopted for the calculation of radiative transfer for the shoulder-expansion region. That is, intensity of radiation is calculated only in the radially inward direction normal to the centerline axis, and the radiation flux is obtained by multiplying the intensity of the normal ray by 2π. The procedure implicitly assumes that the emitting layer is much thinner than the body diameter, and that the medium is optically thin for the Balmer-Paschen lines and continua. The assumptions are believed to lead to an error of the order of 10%, which is acceptable in the present work.

For the three equilibrium regions located along the central axis (recirculating, recompression, and neck regions), an axisymmetric radiative-transport calculation is performed for the base stagnation point. To obtain radiation intensity falling on the stagnation point as a sufficiently fine function of the viewing polar angle, the calculation is performed along 16 different polar angle directions. The first 6 are chosen at especially small angular intervals in order to resolve the rapidly varying contribution of different parts of the neck region. Radiative properties needed in the calculation are obtained using the computer code ARCRAP.[14]

For the case with ablation, preliminary calculation with the code ARCRAP indicates that all molecular radiation is negligible for the benchmark case. This is because temperature is above 10,000 K in all three regions; concentrations of molecules are very small at such high temperatures. Also, oxygen species are seen to contribute negligibly. The only species contributing significantly to radiative transfer, therefore, are hydrogen and carbon species. The radiative properties of hydrogen species are well known. The lines of neutral carbon included in the calculation are: (1) all lines listed in the NBS tables[15] (f numbers given in the tables are used for these lines) and (2) all lines that emanate from an upper state of principal quantum numbers of 5 or less but are missing from the NBS tables (f numbers for these lines are obtained from the corresponding transitions in N^+, O^{++}, or H_e).[16]

Altogether 374 lines of carbon are included. The shape of the carbon lines is taken to be the Voigt profile.[17] The Gaussian component of the Voigt profile is uniquely determined from temperature. The Lorentzian component of the Voigt profile consists of three parts, those corresponding to natural broadening, Stark broadening, and Van der Waals broadening. The width of naturally broadened line is known exactly. All Stark line widths obtained for carbon by Griem[18]

are accommodated. For the lines with unknown Stark line widths, the half-half-width $\Delta\lambda$ is estimated with the formula:

$$\Delta\lambda = 0.025(\lambda/10{,}000)(N_e/10^{16}),\ \text{Å}$$

where N_e is electron density (in cm^{-3}). The formula approximately represents the mean value of all known Stark widths of carbon.[18] The Van der Waals line width is subdivided into two parts, the broadening due to hydrogen atoms and that due to all other atoms and molecules. The reason for this subdivision is that hydrogen atoms induce exceptionally large broadening. The broadening due to hydrogen atom is approximated by

$$\Delta\lambda = 0.02(\lambda/2000)^2([H]/10^{16}),\ \text{Å}$$

where [H] is the concentration of hydrogen atoms (in cm^{-3}). The formula approximately represents the mean values of the line widths for silicon atoms produced by the same mechanism.[14] The approximation is made here because carbon is similar to silicon in spectroscopic properties. The Lorentzian line widths due to broadening by collisions between carbon and all atoms and molecules other than hydrogen are calculated as in the work of Park and Arnold.[19]

The bound-free continua of C and free-free continua of C^+ are calculated using the cross-sectional data of Peach.[20] The photon energies in the range of 0.2 to 16.2 eV are divided into 18,500 equally spaced intervals for this calculation.

No attempt is made to calculate the absorption of radiation from the hot gases by the cold gases adjacent to the wall. Since pressure is low in the base region, absorption by the cold gases is not likely to be significant. Moreover, any reduction in radiative heat-transfer rate due to absorption is likely to be partially compensated for by the rise in convective heat-transfer rate caused by the absorption.

Results

The results of the foregoing calculations are shown in Figs. 3-7. They are given in greater detail in Ref. 21. Figure 3 shows the intensity of the inward radiation flux emerging from the shoulder-expansion region as a function of distance x. At x = 0, the calculated flux value represents approximately 80% of the heat flux in the frustum edge on the forebody side. This is because the initial thickness of the expansion region is taken to be 80% of that of the shock-layer thickness (see section on Shoulder-Expansion Region).

A close examination
that the radiation heat f
same as those from an opt
by

$$e = (2.7 \pm 0.68) \times 1$$

The upper error limit occ
limit pertains to high pr
concern. As evident from
is a function mostly of e
independent of atom densi
well-known effect of none
properties were calculate
densities would be consid
here, leading to correspo
values.[13]

Figure 3 also shows
this region is the strong
than the peak heating poi
This early arrival of the
shoulder-expansion region
flight velocity and chemi
density. The radiation f
cylindrical surfaces surr
the total inward heat flu
value at x = 0 are given

In Figs. 4 and 5, th
reaching the base stagnat
ablating and the ablating
many more lines than Fig.
carbon lines included in t
figures, radiation at phot
weak. This is attributed
the high-energy photons ar
function value is small fo
partly justifies neglectir
adjacent to the wall since
primarily those photons ir

Figure 6 shows the ar
flux received by the base
figure, radiation received
slightly higher (27%) than
ablation. For both cases,
received is in the angular
small angular range is irr

A close examination of the calculated results revealed that the radiation heat flux values are approximately the same as those from an optically thin gas with emissivity given by

$$e = (2.7 \pm 0.68) \times 10^{-32} \, (10{,}000/T_e)^{1.64} \, N_e^2, \ W/cm^3$$

The upper error limit occurs at low pressures, and the lower limit pertains to high pressure within the pressure range of concern. As evident from the expression, radiation intensity is a function mostly of electron density and is virtually independent of atom density. The expression underscores the well-known effect of nonequilibrium.[9,13,22] If the flow properties were calculated assuming equilibrium, electron densities would be considerably smaller than those obtained here, leading to correspondingly small heat-transfer rate values.[13]

Figure 3 also shows that the radiative heat flux q in this region is the strongest at t = 109 sec, which is earlier than the peak heating point for the front stagnation point. This early arrival of the peak heating point for the shoulder-expansion region is caused by the combination of high flight velocity and chemical nonequilibrium caused by low density. The radiation flux q is integrated over the cylindrical surfaces surrounding the frustum edge to obtain the total inward heat flux. The results and the maximum q value at x = 0 are given in Table 1.

In Figs. 4 and 5, the spectra of the radiation fluxes reaching the base stagnation point are shown for the non-ablating and the ablating cases, respectively. Figure 5 shows many more lines than Fig. 4. The difference is due to atomic carbon lines included in the calculation for Fig. 5. In both figures, radiation at photon energies greater than 10 eV are weak. This is attributed to the combination of two facts: the high-energy photons are self-absorbed and the blackbody-function value is small for the high-energy range. This fact partly justifies neglecting absorption by the cold gases adjacent to the wall since absorption would attenuate primarily those photons in the high-energy range.

Figure 6 shows the angular distribution of radiation flux received by the base stagnation point. As seen in the figure, radiation received in the case with ablation is slightly higher (27%) than that received in the case without ablation. For both cases, over half the total radiation received is in the angular range of $0 < \theta < 0.6$ rad. This small angular range is irradiated primarily by the radiation

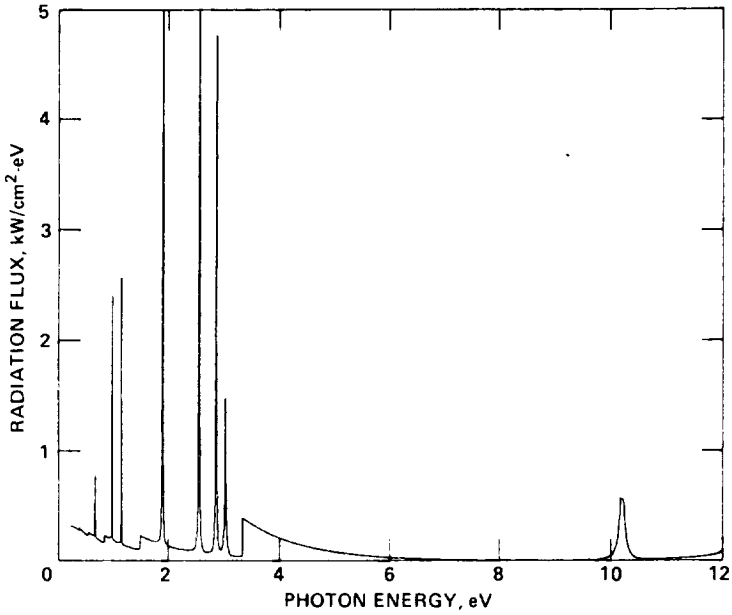

Fig. 4 Calculated spectra of radiation flux at base stagnation-point at benchmark point, without ablation.

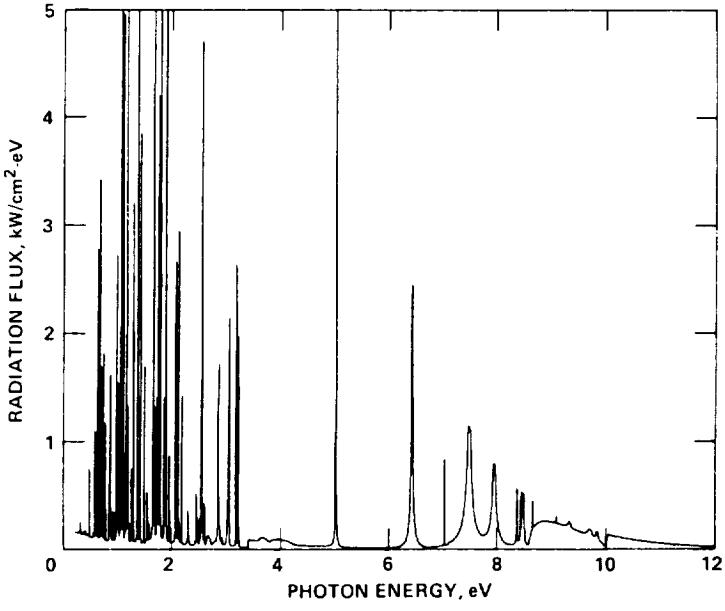

Fig. 5 Calculated spectra of radiation flux at base stagnation-point at benchmark point, with ablation.

emitted by the neck and re
the figure. By integratir
obtains the total radiatic
point given in Table 1.

Figure 7 a shows the
$\oint q\, dA$ from the shoulder-e
along the entry trajector
over the surface of the ir
schematically in Fig. 7 a
because it was thought to
the heat-shield design.
transfer rate for the base
function of time. For th
occurs only slightly ahea
front stagnation point.
7 b leads to $\int q\, dt = 1.4$

The results just sho
radiative heating of the
behind the frustum. This
the same radiative heatinc
luminosity persists behinc
region, partly because of

The radiative heatinc
is substantially greater
Its absolute value is onl
and without ablation (the
larger) even though the s
circulating, recompressior
colder when ablation produ
difference between the tw
that carbon radiates more
hydrogen.

Several assumptions
the present theory, the m
be the value for base pre
based on an average base
pressure or, equivalently
pressure. In order to in
pressure, calculations we
pressure values for the b
The results show that the
rate q is approximately p
to-front stagnation-point

emitted by the neck and recompression regions as indicated in the figure. By integrating under the curves in Fig. 6, one obtains the total radiation flux q for the base stagnation point given in Table 1.

Figure 7 a shows the area-integrated radiation power $\oint q\, dA$ from the shoulder-expansion region as a function of time along the entry trajectory. The areal integration here is over the surface of the imaginary semi-infinite cylinder shown schematically in Fig. 7 a . The quantity is shown here because it was thought to be more useful than the q values in the heat-shield design. In Fig. 7 b , the radiative heat-transfer rate for the base stagnation point is shown as a function of time. For this case, the peak heating point occurs only slightly ahead of the peak heating point for the front stagnation point. Integrating under the curve in Fig. 7 b leads to $\int q\, dt = 1.4 \times 10^4$ J/cm^2.

Discussion

The results just shown indicate that the most severe radiative heating of the base region would occur immediately behind the frustum. This region is subject approximately to the same radiative heating as the forebody. Relatively high luminosity persists behind the frustum in the expansion region, partly because of the nonequilibrium effect.

The radiative heating rate of the base stagnation point is substantially greater than the convective heating rate.[5] Its absolute value is only slightly different in cases with and without ablation (the ablating case value is 1.27 times larger) even though the sources of radiation (i.e., the re-circulating, recompression, and neck regions) are appreciably colder when ablation products are present. Such a small difference between the two cases can be attributed to the fact that carbon radiates more strongly at low temperatures than hydrogen.

Several assumptions have been made in the development of the present theory, the most important of which is believed to be the value for base pressure. The present calculations are based on an average base pressure that is 4.5% of the frustum pressure or, equivalently, 2.3% of the front stagnation-point pressure. In order to investigate the possible effect of base pressure, calculations were made with two different base-pressure values for the benchmark condition (t = 111.3 sec). The results show that the base stagnation-point heat-transfer rate q is approximately proportional to the square of the base-to-front stagnation-point pressure ratio p_b/p_s. For the

Table 1 Summary of heat-transfer rate q calculations

Forebody data (Moss[6] solutions)						
Trajectory point	612	652	685	703	726	748
Time, sec	99.5	103.9	107.2	109.0	111.3	113.5
Altitude, km	195.6	169.6	149.1	138.6	126.1	115.3
Freestream density, g/cm^3, $\times 10^8$	2.65	7.19	16.4	24.5	43.6	70.2
Flight velocity, km/sec	48.07	46.96	44.83	42.88	39.29	34.67
Front stagnation-point pressure, atm	0.56	1.44	2.97	4.20	6.01	7.45
Front stagnation point q, without ablation						
Convective, kW/cm^2	7.90	11.4	14.0	14.8	14.7	12.8
Radiative, kW/cm^2	2.70	10.2	25.0	35.3	42.3	32.0
Front stagnation point q, with ablation						
Convective, kW/cm^2	...	...	...	...	0.02	...
Radiative, kW/cm^2	...	...	...	...	19.4	...
Afterbody data (radiative only)						
Shoulder-expansion region						
Max q, kW/cm^2	0.82	3.42	6.66	7.48	4.47	1.98
$\oint q\, dA$, MW	3.22	13.5	24.8	25.5	13.5	1.04
Base stagnation point q						
Without ablation, kW/cm^2	0.091	0.391	1.02	1.45	1.72	1.27
With ablation, kW/cm^2	...	...	...	...	2.19	...

Fig. 6 Angular dist
stagnation-point fo

benchmark case with abl
front stagnation-point

$$q/q_s$$

Assuming that the ratio
without ablation applie
estimate of the heat lo
calculated trajectory b

$$\int q\, dt = 1.8$$

The present analys
concerns only the two e
shield — the base stag
treme outer edge. The
core regions (i.e., rec
regions) and the outer
expansion region. An i
two extreme positions w
sources of radiation.

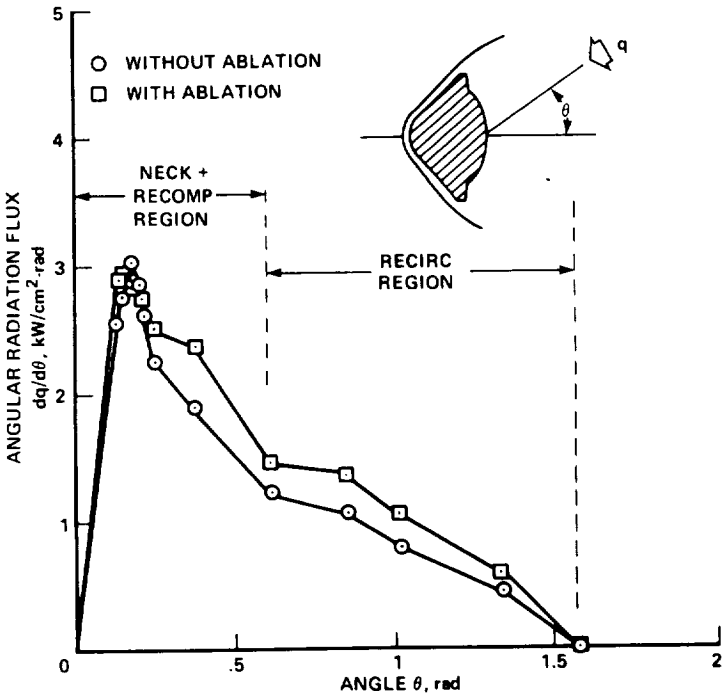

Fig. 6 Angular distribution of radiation flux at base stagnation-point for benchmark point.

benchmark case with ablation, therefore, the ratio of base-to-front stagnation-point heat-transfer rate becomes

$$q/q_s = 0.113(43.4p_b/p_s)^2$$

Assuming that the ratio of 1.27 between the cases with and without ablation applies at all trajectory points, the best estimate of the heat load to the stagnation point for the calculated trajectory becomes

$$\int q\,dt = 1.8 \times 10^4(43.4p_b/p_s)^2,\ J/cm^2$$

The present analysis of radiative heat-transfer rate concerns only the two extreme positions on the base heat shield — the base stagnation point (axis-point) and the extreme outer edge. The base stagnation point is heated by the core regions (i.e., recirculating, recompression, and neck regions) and the outer edge is irradiated by the shoulder-expansion region. An intermediate, off-axis point between the two extreme positions will be subject to heating from both sources of radiation. The intensity of radiation cast by the

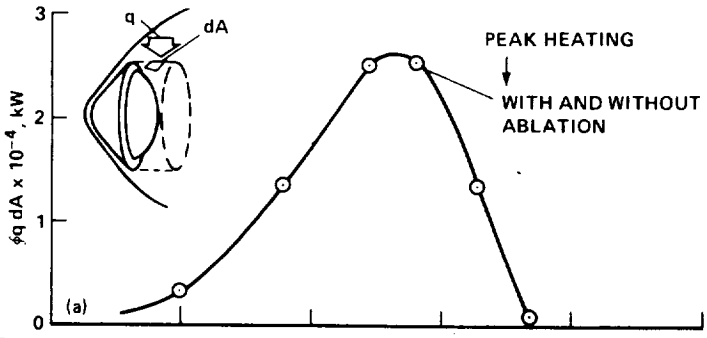

a) Integrated heat load from shoulder-expansion region.

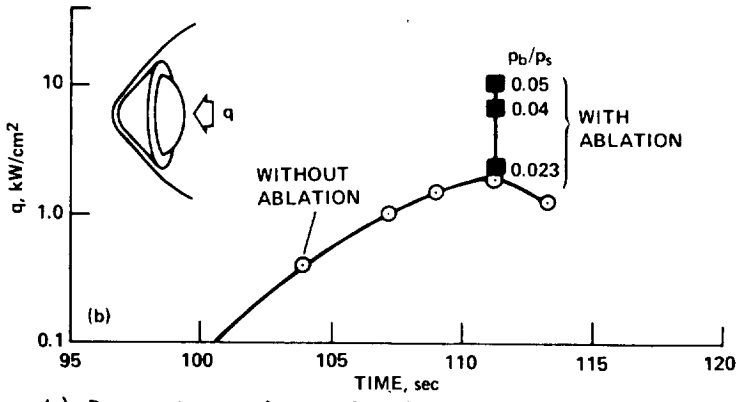

b) Base stagnation-point heat-transfer rate.

Fig. 7 Heat load in base region.

three core regions on the off-axis point will be approximately the same as that on the axis point. The average distance from the recirculating region to the off-axis point is slightly farther than to the axis point, but its effect is offset by the fact that the viewing angle of the neck region is larger. Since the off-axis point is at an oblique angle to the normal plane, the heating rate will be lower by the cosine of the angle. This slight reduction will be offset by the added heating from the shoulder-expansion region. As a result, the off-axis point will be subject essentially to the same or slightly greater radiative heating than the base stagnation point. The experimental data of Shirai and Park[4] taken at an off-axis point confirms this trend.

The present analysis entails a scale effect for the shoulder-expansion region. The flow in the region will tend to freeze chemically when the body size becomes small, thereby

producing large electr
radiation power. But
rate is virtually inde
sources of radiation (
regions) are in equili
the luminous regions a
contradicts the argume
base stagnation-point
body size. Stephenson
observations made at r
low Reynolds number re
predict a size-depende
average total enthalpy
layer will depend on R
number is greater than
average enthalpy becom
number since the volum
shear layer will be de
parameter alone, which
the Jovian flight case
Shirai and Park,[4] the
is believed to be in t
is unaffected by the R

Radiative heating
frustum on a Jovian en
equilibrium expansion
significant. The base
recirculating, recompr
recompression and neck
The base stagnation-po
slightly greater in th
absence. Near the pea
point heating rate is
volume-averaged pressu
ratio to the front sta
and the time-integrate

Sincere thanks ar
group at Ames Research
C. E. De Rose, and the
flight experiment.

producing large electron density values and hence large radiation power. But the base stagnation-point heat-transfer rate is virtually independent of size because the three sources of radiation (recirculating, recompression, and neck regions) are in equilibrium and because the viewing angles of the luminous regions are independent of size. This conclusion contradicts the argument of Stephenson[2] which predicts the base stagnation-point heat-transfer rate to be dependent on body size. Stephenson's argument is based on experimental observations made at relatively low Reynolds numbers. In a low Reynolds number regime, the present theory will also predict a size-dependent heat-transfer rate because the average total enthalpy of the flow entrained by the free-shear layer will depend on Reynolds number. When the Reynolds number is greater than a certain critical value, however, the average enthalpy becomes virtually independent of Reynolds number since the volume of the mass entrained by the free-shear layer will be determined by the shear-spreading parameter alone, which is approximately constant.[5] In both the Jovian flight case and the experimental conditions of Shirai and Park,[4] the Reynolds number is relatively high and is believed to be in the regime where the heat-transfer rate is unaffected by the Reynolds number.

Conclusions

Radiative heating is most severe immediately behind the frustum on a Jovian entry probe. Radiation from the non-equilibrium expansion region downstream of the frustum is also significant. The base stagnation point is irradiated by the recirculating, recompression, and neck regions, with the recompression and neck regions contributing the major portion. The base stagnation-point radiative heat-transfer rate is slightly greater in the presence of ablation than in its absence. Near the peak heating point, the base stagnation-point heating rate is $2.2(43\ p_b/p_s)^2$ W/cm^2 where p_b is the volume-averaged pressure in the recirculating region. Its ratio to the front stagnation-point value is $0.11(43p_b/p_s)^2$, and the time-integrated heat load is $18(43p_b/p_s)^2$ kJ/cm^2.

Acknowledgments

Sincere thanks are extended to the hypersonic free-flight group at Ames Research Center — D. B. Kirk, P. F. Intrieri, C. E. De Rose, and their associates — for conducting the free-flight experiment.

References

[1]Lockman, W. K., "Free-Flight Base Pressure and Heating Measurements on Sharp and Blunt Cones in a Shock Tunnel," AIAA Journal, Vol. 5, Oct. 1967, pp. 1898-1900.

[2]Stephenson, J. D., "Measurement of Optical Radiation from the Wake of Ablating Blunt Bodies in Flight at Speeds up to 10 km per Second," NASA TN D-2760, April 1965.

[3]Stephenson, J. D., "Measured and Predicted Ablation-Product Radiation in the Near Wake," Fluid Physics of Hypersonic Wakes, AGARD Specialist's Meeting on Fluid Physics of Hypersonic Wakes, Vol. 2, Colorado State Univ., Fort Collins, Colo., May 1967.

[4]Shirai, H. and Park, C., "Experimental Studies of Radiative Base Heating to a Jovian Entry Model," AIAA Paper 79-0038, Jan. 1979.

[5]Nestler, D. E. and Brant, D. N., "Development of an Afterbody Radiative and Convective Heating Code for Outer Planet Probes," AIAA Paper 78-862, May 1978.

[6]Moss, J. N., Anderson, E. C., and Simmonds, A. L., "The Impact of Turbulence on a Radiating Shock Layer," AIAA Paper 78-1186, July 1978.

[7]Weng, C. H. and Chow, W. L., "Axisymmetric Supersonic Turbulent Base Pressures," AIAA Journal, Vol. 16, June 1978, pp. 553-554.

[8]Murthy, S. N. B. and Osborn, J. R., "Base Flow Phenomena With and Without Injection: Experimental Results, Theories, and Bibliography," Progress in Astronautics and Aeronautics: Aerodynamics of Base Combustion, Vol. 40, edited by S. N. B. Murthy, AIAA, New York, 1976, pp. 7-210.

[9]Park, C., "Comparison of Electron and Electronic Temperatures in Recombining Nozzle Flow of Ionized Nitrogen-Hydrogen Mixture, Part 1, Theory," Journal of Plasma Physics, Vol. 9, Pt. 2, Feb. 1973, pp. 187-215.

[10]Marvin, J. G. and Kussoy, M., "Experimental Investigation of the Flow Field and Heat Transfer Over the Apollo-Capsule Afterbody at a Mach Number of 20," NASA TM X-1032, Feb. 1965.

[11]Lees, L. and Hromas, L., "Turbulent Diffusion in the Wake of a Blunt-Nosed Body at Hypersonic Speeds," Journal of the Aerospace Sciences, Vol. 29, Aug. 1962, pp. 976-993.

[12]Chapman, D. R., Kuehn, D
tion of Separated Flows ir
with Emphasis on the Effec
1957.

[13]Park, C., "Calculation c
equilibrium Hydrogen Plasm
Spectroscopy and Radiative
pp. 101-112.

[14]Prakash, S. G., and Park
Silicon Emission in the Sp
Paper 78-234, Jan. 1978.

[15]Wiese, W. L., Smith, M.
Transition Probabilities,
National Bureau of Standa
Printing Office, May 1966

[16]Wilson, K. H. and Nicol
efficients of Carbon, Nit
Quantitative Spectroscopy
Nov./Dec. 1967, pp. 891-9

[17]Richter, J., "Radiation
edited by W. Lochte-Holtg
1968, pp. 1-65.

[18]Griem, H. R., Plasma Sp
1964.

[19]Park, C. and Arnold, J.
the SiO($A^1\pi$-$X^1\Sigma^+$) Transit
Spectroscopy and Radiativ
pp. 1-10.

[20]Peach, G., "Continuous
Hydrogenic Atoms," Memoir
Vol. 72, Pt. 1, 1970, pp.

[21]Park, C., "Modeling of
Jovian Entry Probe," AIAA

[22]Bates, D. R., Kingston,
"Recombination Between El
Thin Plasmas," Proceeding
A267, May 1962, pp. 297-3

[12]Chapman, D. R., Kuehn, D. M., and Larson, H. K., "Investigation of Separated Flows in Supersonic and Subsonic Streams with Emphasis on the Effect of Transition," NACA Rept. R-1356, 1957.

[13]Park, C., "Calculation of Radiative Properties of Non-equilibrium Hydrogen Plasma," Journal of Quantitative Spectroscopy and Radiative Transfer, Vol. 22, July 1979, pp. 101-112.

[14]Prakash, S. G., and Park, C., "Shock Tube Studies of Atomic Silicon Emission in the Spectral Range 180 to 300 nm," AIAA Paper 78-234, Jan. 1978.

[15]Wiese, W. L., Smith, M. W., and Glennon, B. M., Atomic Transition Probabilities, Vol. 1, Hydrogen Through Neon, National Bureau of Standards, NSRDS-NBS 4, U. S. Government Printing Office, May 1966.

[16]Wilson, K. H. and Nicolet, W. E., "Spectral Absorption Coefficients of Carbon, Nitrogen, and Oxygen Atoms," Journal of Quantitative Spectroscopy and Radiative Transfer, Vol. 7, Nov./Dec. 1967, pp. 891-941.

[17]Richter, J., "Radiation from Hot Gases," Plasma Diagnostics, edited by W. Lochte-Holtgreven, North-Holland, Amsterdam, 1968, pp. 1-65.

[18]Griem, H. R., Plasma Spectroscopy, McGraw-Hill, New York, 1964.

[19]Park, C. and Arnold, J. O., "A Shock-Tube Determination of the SiO($A^1\pi$-$X^1\Sigma^+$) Transition Moment," Journal of Quantitative Spectroscopy and Radiative Transfer, Vol. 19, Jan. 1978, pp. 1-10.

[20]Peach, G., "Continuous Absorption Coefficients for Non-Hydrogenic Atoms," Memoirs of the Royal Astronomical Society, Vol. 72, Pt. 1, 1970, pp. 1-123.

[21]Park, C., "Modeling of Radiative Heating of Base Region of Jovian Entry Probe," AIAA Paper 79-0039, Jan. 1979.

[22]Bates, D. R., Kingston, A. E., and McWhirter, R. W. P., "Recombination Between Electrons and Atomic Ions, I. Optically Thin Plasmas," Proceedings of the Royal Society (London), Vol. A267, May 1962, pp. 297-312.